Evaluation of L-Methioninase as a Targeted Anticancer Agent in Colorectal Cancer and Renal Cell Carcinoma

Abbas Abed Noor Al-Owaidi*, Mohammed Abdullah Jebor

Department of Biology, College of Sciences, University of Babylon, Babylon, Hillah, 51001, Iraq

Received: Jan. 2025; Accepted: Mar. 2025

Abstract- The employment of L-Methioninase (L-Met), an enzyme degrading L-methionine, as a possible anticancer therapy has been provided that it selectively destroys cancer cells, which require methionine to grow. Many tumor tissues have a limited capacity for methionine production and depend on exogenous supplies of this amino acid. Therefore, they could be selectively attacked by methioninase-based treatment. The present study was carried out to investigate the effect of L-Met on cancer cells, especially colorectal cancer (HCT-116) and renal cell carcinoma (A498), and its potential as a therapeutic agent. Various techniques, such as ammonium sulfate precipitation, dialysis, ion-exchange chromatography, and gel filtration chromatography, were employed in this study for enzyme purification of L-Met. Cytotoxicity testing was performed against HCT-116 and A498 cells in the range of 25-200 µg/mL concentration by the MTT assay for viable cell quantification, Total Nuclear Intensity (TNI), and Cell Membrane Permeability (CMP). The statistical analysis was done using one-way ANOVA and Dunnett's multiple comparisons test to compare multiple groups. The optimal temperature for enzyme activity was 37° C, with pH 7 offering the best enzyme stability. Further investigation into incubation time revealed that a 48-hour period maximized enzyme yield. The enzyme was purified using a combination of ammonium sulfate precipitation, ion-exchange chromatography, and gel filtration, achieving a 4.6-fold increase in purity. Characterization of the purified enzyme revealed a molecular weight of approximately 55 kDa, with optimal activity at pH 7 and 37°C. The enzyme demonstrated strong potential for therapeutic applications, showing dose-dependent cytotoxicity against colorectal cancer (HCT-116) and renal cancer (A498) cell lines, with significant inhibitory effects at concentrations as low as 25 µg/mL for colorectal cancer cells. The study highlights the potential of *P. aeruginosa*-derived L-Met showed strong activity in colorectal cancer, while activity in renal cell carcinoma was lower or inconclusive.

Acta Med Iran 2025;63(March-April):73-82.
https://doi.org/10.18502/acta.v63i2.18961

Keywords: L-met; Pseudomonas aeruginosa; Colorectal cancer; Renal cell carcinoma

Introduction

Cancer remains one of the leading causes of morbidity and mortality worldwide, with colorectal cancer (CRC) and renal cell carcinoma (RCC) being two of the most prevalent and aggressive forms of malignancies (1). Despite advancements in early detection and therapeutic strategies, both CRC and RCC present significant treatment challenges due to their heterogeneity, resistance to conventional therapies, and high potential for metastasis (2). There is an urgent need for novel, targeted therapies that can specifically disrupt cancer cell metabolism and offer better therapeutic outcomes with fewer side effects (3).

In this context, one promising candidate for targeted anticancer therapy is L-methioninase (L-Met), an enzyme that catalyzes the degradation of methionine, an essential amino acid (4). Methionine is crucial for protein synthesis, methylation reactions, and cellular metabolism. However, many cancer cells exhibit an increased dependence on methionine due to their heightened metabolic demands for rapid growth and

Corresponding Author: A.A. Noor Al-Owaidi
Department of Biology, College of Sciences, University of Babylon, Babylon, Hillah, 51001, Iraq
Tel: +9647705713626, E-mail address: alowaidiabbas47@gmail.com

proliferation. This phenomenon, known as "methionine dependence," provides a unique opportunity to exploit L-Met as a therapeutic agent (5,6).

L-Met has garnered attention for its potential as an anticancer agent due to its ability to specifically deplete methionine levels in the tumor microenvironment, thereby impairing cancer cell growth and survival (4). By lowering methionine availability, L-Met disrupts various cellular processes, including DNA and RNA synthesis, methylation of critical regulatory proteins, and cellular redox homeostasis, all essential for cancer cell proliferation (7). Moreover, L-Met has shown the potential to selectively target tumor cells over normal cells, given that normal cells can often compensate for lower methionine levels through alternative metabolic pathways. This selectivity makes L-Met an attractive option for targeted cancer therapy, potentially offering a therapeutic approach with reduced toxicity compared to traditional chemotherapies (8).

The applicability of L-Met as a therapeutic agent has been explored in various cancer types, with promising results in preclinical models and early-phase clinical trials (4). In particular, its potential in treating CRC and RCC has been of significant interest. CRC is one of the leading causes of cancer-related deaths, and although treatment strategies have evolved, metastatic disease remains a major challenge (9). RCC, similarly, is a highly aggressive cancer that often presents at an advanced stage and is known for its resistance to many standard treatments, including chemotherapy and radiation. Therefore, the development of novel, effective therapies for both these cancers is critical (10).

The rationale for targeting methionine metabolism in CRC and RCC lies in the metabolic reprogramming these tumors undergo to sustain rapid growth (11). In CRC, alterations in the methionine cycle and key regulatory pathways such as the mTOR and PI3K-Akt signaling pathways contribute to the dysregulation of cellular metabolism and promote tumorigenesis (12).

In RCC, mutations in the von Hippel-Lindau (VHL) gene stabilize hypoxia-inducible factors (HIFs), further enhancing tumor cells' metabolic demands (13). Both cancers exhibit a heightened reliance on methionine, and reducing methionine availability through L-Met could potentially lead to significant therapeutic benefits by disrupting these metabolic pathways (11).

While L-Met shows promise in preclinical studies, several challenges remain in translating its potential into clinical success. Issues such as the stability of the enzyme, its delivery to tumors, and the need for optimal dosing regimens must be addressed to maximize its efficacy (14). Furthermore, combining L-Met with other therapeutic agents, such as chemotherapy, targeted therapies, or immune checkpoint inhibitors, could enhance its anticancer effects and offer more robust treatment options for CRC and RCC patients (4). Therefore, the present study aims to critically evaluate the current evidence surrounding the use of L-Met as a targeted anticancer agent in colorectal cancer and renal cell carcinoma.

Materials and Methods

Sample collection

A total of 150 clinical samples were collected randomly from UTI, burns, sputum infection, wound, and otitis media patients hospitalized in Baghdad Hospital. All samples were transferred under sterile conditions and maintained at 4° C during transport. The time between sample collection and laboratory processing did not exceed 2 hours.

Buffer preparation

The following buffers were used to maintain a certain pH in the enzyme activity assay: potassium phosphate buffer (0.5 M, pH 7), Tris-HCl buffer (0.05 M, pH 7), and Tris-base buffer (0.1 M, pH 8 and 9). Certain other solutions, including sodium chloride (0.25 M), sodium hydroxide (0.25 M), and hydrochloric acid (0.25 M), were prepared for purification.

Isolation and identification of pseudomonas aeruginosa

The samples were cultured in brain heart infusion broth and subjected to general and differential culture techniques. Colonies of *P. aeruginosa* were identified by colonies on lactose non-fermenting MacConkey agar and cetrimide agar. Cetrimide agar was specifically used to assess the production of pyocyanin and fluorescein. Pigment production was confirmed visually based on colony coloration-pyocyanin appeared as a characteristic blue-green pigment, while fluorescein exhibited a yellow-green hue. To confirm fluorescein production, plates were also examined under UV light (365 nm), where a distinct green fluorescence indicated its presence. No spectrophotometric quantification was performed at this stage, as the purpose was preliminary qualitative screening. Biochemical tests such as oxidase, catalase, indole, utilization of citrate, and production of urease confirmed the bacterial identification.

L-Met activity assay

The Nesslerization method was used to assay the activity of L-Met. A reaction mixture containing 1% L-methionine, potassium phosphate buffer (0.5 M, pH 7), pyridoxal phosphate (PLP), and crude enzyme was incubated at 30° C for 1 hour. This method is highly sensitive for detecting ammonia, and appropriate controls were included to account for potential interfering substances in the crude enzyme extract. The reaction was stopped with trichloroacetic acid, and the ammonia release was assessed with Nessler reagent. The enzyme-specific activity was expressed as µmol of ammonia produced/ min/mg protein.

Protein concentration determination

Bradford's method quantified the concentrated protein (Bradford Reagent, Bio-Rad, USA). The absorbance was measured at 595 nm, and a standard curve was generated with bovine serum albumin (BSA) (BSA; Sigma-Aldrich, USA).

Purification of L-met

Ammonium sulfate precipitation

The crude enzyme extract was subjected to ammonium sulfate (HiMedia, India) precipitation at different saturation levels: 30%, 40%, 50%, 60%, 70%, and 80%. The mixture was centrifuged at 6,000 rpm for 6 hours at 4° C using a refrigerated centrifuge (Eppendorf 5810 R, Germany). The fraction precipitated at 70% saturation showed maximum enzyme activity.

Dialysis

The precipitated enzyme was dialyzed through a dialysis membrane (MWCO 3,500 Da; Sigma-Aldrich, USA) against potassium phosphate buffer (pH 7) at 4° C for 24 hours with several buffer changes.

Ion-exchange chromatography

Further target purification was performed by using DEAE cellulose resin. The enzyme solution was applied to the DEAE-cellulose column (Whatman DE52, GE Healthcare, USA), and washed with phosphate buffer. Proteins were eluted with stepwise gradients of sodium chloride, 0.1 M, and 1 M. Enzyme activity and protein concentration for each fraction were assayed.

Gel filtration chromatography

In the final step, Sephadex G-150 gel filtration chromatography (GE Healthcare, USA) was performed. The enzyme was applied to a pre-equilibrated column, and fractions were collected. For each enzyme activity, protein concentration was determined.

Enzyme characterization

Optimum pH and temperature

The optimum pH of L-Met was determined using buffers with different pH ranges from pH 4 to 9, while the temperature stability was investigated at a series of temperatures ranging from 10° C to 60° C. Activities were measured from the substrate degradation at every condition.

Kinetic parameters

The enzyme's kinetic parameters, Km (Michaelis constant) and Vmax (maximum reaction velocity), were determined from Lineweaver-Burk plots using activities at various substrate concentrations.

Cytotoxicity assay

Cell line culturing

Cytotoxicity of L-Met was tested on six cancer cell lines: HCT-116 (colorectal cancer) and A498 (renal cell carcinoma). Cells were cultured in RPMI-1640 medium supplemented with 10% fetal bovine serum, 100 IU/mL penicillin, and 100 µg/mL streptomycin.

MTT assay

Tumor cells were seeded in a 96-well plate ($1x10^4$-$1x10^6$ cells/mL) and incubated for 24 hours with serial dilutions of the enzyme at concentrations ranging from 25-400 µg/m. MTT solution was added to each well after incubation, followed by a further incubation period of 4 hours. The purple-colored formazan crystals that resulted from the reduction were dissolved in a solution for solubilization and then measured at 575 nm using an ELISA microplate reader (BioTek ELx800, USA). Calculation of the IC_{50} was based on the concentration of the enzyme exhibiting 50% inhibition of cell viability.

Statistical analysis

Data was statistically analyzed using one-way ANOVA with Duncan's test to assess significance ($P \leq 0.05$). Results were expressed as mean±standard deviation. All statistical analyses were performed using GraphPad Prism 9.4 software.

Results

Optimum conditions of bacterial isolates for L-Met enzyme production

Optimum carbon sources

To find the best carbon source for *P. aeruginosa's* production of L-Met, various carbon sources—such as

glucose, sucrose, maltose, xylose, and galactose—were investigated as the only energy and carbon sources. The enzymes' specific activity (U/mg protein) when cultivated with different carbon sources is shown in Figure 1. The following are the outcomes:

Sucrose was found to be the most effective carbon source for enzyme synthesis, as evidenced by its greatest specific activity of 1.2 U/mg protein. Maltose exhibited the lowest enzyme activity of all the carbon sources evaluated, with a specific activity of 0.25 U/mg protein. More enzyme activity was observed with xylose than with maltose, showing a specific activity of 0.4 U/mg protein. The specific activity of glucose was 0.45 U/mg protein, which was better than that of xylose. Enzyme activity significantly increased with galactose, showing a specific activity of 1 U/mg protein.

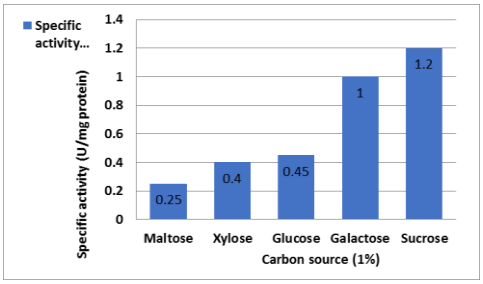

Figure 1. Optimal carbon source for L-Met production from Pseudomonas aeruginosa after incubation at 37° C for 48 hr

Optimum nitrogen sources

Tryptone, peptone, NH4Cl, yeast extract, and casein were investigated to identify the best nitrogen supply. Each nitrogen source was introduced to the medium separately at a concentration of 1% (w/v) to assess its impact on enzyme production.

Figure 2 shows the specific activity of enzymes when cultivated with different nitrogen sources and is expressed in U/mg protein. Tryptone is the most efficient nitrogen source for enzyme synthesis in this investigation, as evidenced by its greatest specific activity of 2.6 U/mg protein. NH4Cl shows a specific activity of 0.8 U/mg protein compared to other nitrogen sources, indicating lesser enzyme activity.

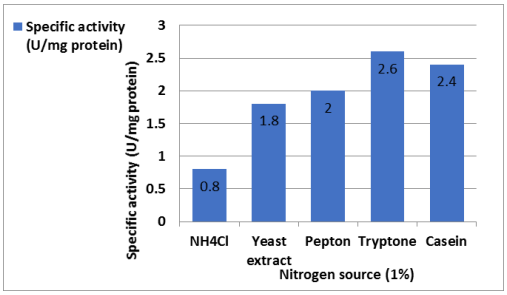

Figure 2. Optimal nitrogen source for L-Met production from Pseudomonas aeruginosa A6 after incubation at 37°C for 48 hr

Optimum temperature

From 10° C to 60° C, enzyme activity increased with temperature, peaking at 1.5 U/mL at 37° C. However, activity declined at higher temperatures, dropping to 0.9 U/mL at 42° C and 0.5 U/mL at 47° C. Similarly, specific activity — indicating enzyme efficiency per mg of protein — peaked at 2.7 U/mg at 37° C and decreased to 0.9 U/mg at 42° C, suggesting diminished efficiency at elevated temperatures (Figure 3).

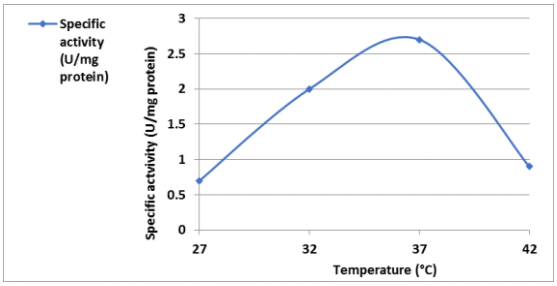

Figure 3. Effect of temperature on the specific activity of L-Met enzyme

Optimum PH

The pH range in which the L-Met exhibited optimal activity was 4 to 9. According to the findings, the enzyme's activity decreases at more acidic and alkaline pH values and peaks at pH 7. Additionally, the data demonstrates that the enzyme's stability and activity are highest at pH 7 and 8, with a discernible decline at both acidic and extremely alkaline pH levels (Figure 4).

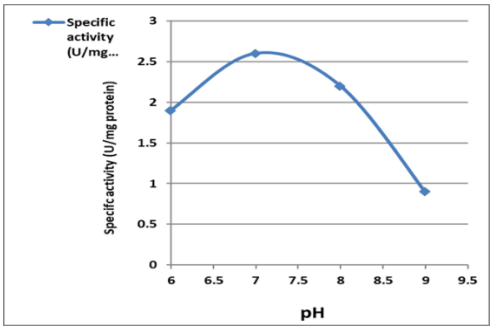

Figure 4. Optimal pH for L-Met production from Pseudomonas aeruginosa A6 after incubation at 37°C for 48 hr

Optimal incubation period

Over 48 hours, the enzyme's specific activity rose to a maximum of 3.3 U/mg protein. Nevertheless, after 72 hours, the specific activity dropped to 2.5 U/mg protein,

suggesting a reduction in enzyme efficiency with extended incubation (Figure 5).

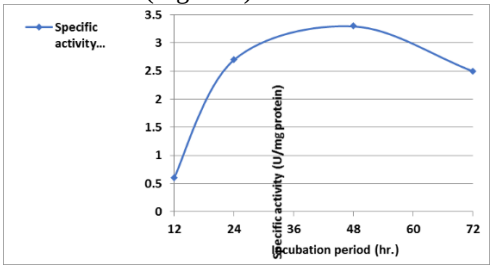

Figure 5. The optimal incubation period for P. aeruginosa producing L-Met at 37° C Purification of L-Met

Three purification procedures were used to purify the L-Met that *Pseudomonas aeruginosa* produces best. These phases included:

Precipitation of L-met by ammonium sulfate

After that, a 30%-80% ammonium sulfate precipitation was applied to the crude enzyme solution. The optimal condition for preserving enzyme activity was 70% saturation, which yielded the highest enzyme activity (4.5 U/ml) and specific activity (11.2 U/mg protein) (Table 1).

Table 1. Enzyme Activity and Specific Activity of L-Met at Different Ammonium Sulfate Saturations

Ammonium sulfate (%)	Activity (U/ml)
30	0.9
40	1.5
50	2
60	4
70	4.5
80	3.8

Ion-exchange chromatography

The DEAE-cellulose resin was utilized to purify the enzyme further. Protein content and activity were measured after the enzyme fractions were eluted using sodium chloride gradients (0.1 M to 1 M). An ion-exchange chromatography (IEC) method divides ionizable molecules according to variations in their charge characteristics. This procedure involved measuring the collected fractions' optical density (OD) at 280 nm using a spectrophotometer. A single protein peak was produced in the washing step, where potassium phosphate buffer was used to elute positively charged fractions. The washing process was repeated until the OD values dropped to zero, meaning no more positively charged proteins were in the column.

Another peak was obtained during the elution step, which involved introducing a gradient of sodium chloride concentrations to liberate the negatively charged proteins attached to the column. The eluted fractions (59 to 66) contained the majority of the L-Met activity. With a purification fold 2.6 and an overall yield of 48%, the enzyme's specific activity in these fractions was 10.7 U/mg protein.

Gel filtration chromatography

The last purification step, Sephadex G-150 gel filtration, gave the fractions the protein concentration and enzyme activity data that they needed to be successfully isolated. L-Met was purified by the gel filtering stage using Sephadex G-150, resulting in a high specific activity of 16.6 U/mg and a notable 4.6-fold increase in purity. However, compared to other approaches, its recovery yield (45%) was slightly lower (Table 2).

Table 2. Purification procedures for L-Met production from Pseudomonas aeruginosa

Purification step	Volume (ml)	Enzyme activity (U/ml)	Protein concentration (mg/ml)	Specific activity (U/mg)	Total activity (U)	Purification (folds)	Yield (%)
Crude enzyme	70	1	0.3	3.3	70	1	100
Ammonium sulphate precipitation (70%)	11	4.5	0.4	11.2	49.5	3.4	70.7
DEAE-cellulose	21	2.2	0.1	22	46.2	6.6	66
Sephadex- G150	21	1.5	0.09	16.6	31.5	5	45

Characterization of purified L-met enzyme

Effect of PH on enzyme activity and stability

The relationship between pH and enzyme activity, expressed in units per milliliter (U/mL), is shown in Fig. 9. The maximal enzyme activity of 1.5 U/mL was observed at pH 7, and it fell at both more basic (pH 9) and more acidic (pH 5) conditions. Additionally, the enzyme's activity gradually declines at higher basic (pH 9 and 10) and acidic (pH 5) pH values, with the best structural stability occurring at pH 7 and 8. This implies that the pH range close to neutral is where the enzyme's structure is most stable (Figure 6).

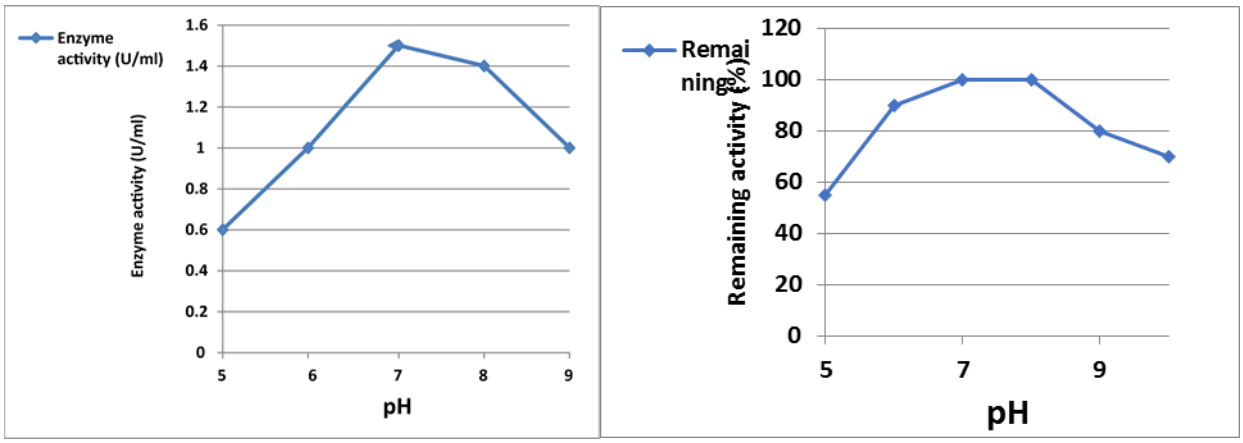

a b

Figure 6. a) Effect of different pH on the Enzyme specific activity. b) Effect of different pH on the Enzyme structure stability

Effect of temperature on enzyme activity and stability

The link between temperature and enzyme activity, expressed in units per milliliter (U/ml), is shown in Figure 7. The enzyme has an ideal temperature of 37° C for maximum activity, as evidenced by the fact that enzyme-specific activity peaks at this temperature and falls both below and above it. The percentage of residual enzyme activity in Figure 3-13 illustrates how temperature affects the structural stability of enzymes. At 32° C and 37° C, the enzyme retains its maximal structural stability. Enzyme stability declines when the temperature rises over 37° C, with notable drops in activity noted at temperatures beyond 42° C. This implies the enzyme loses structural integrity as temperatures rise and is most stable between 32° C and 37° C.

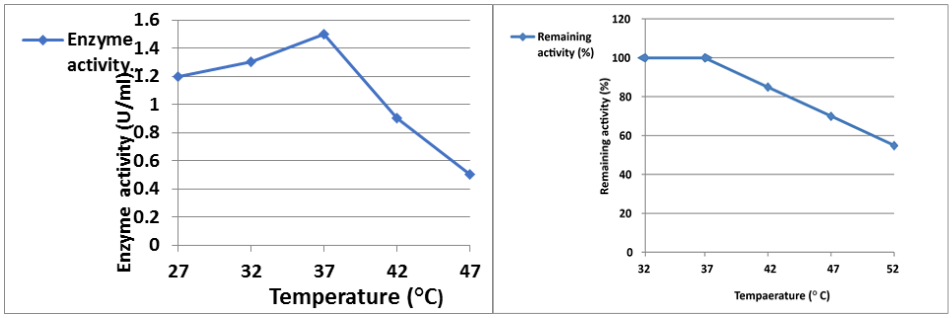

a b

Figure 7. a) Optimum Temperature for Enzyme-Specific Activity. b) Optimum Temperature for Enzyme structure stability

Enzyme-kinetic characterization of L-met enzyme activity

Km and Vmax values, as obtained from Lineweaver-Burk plots, represent the enzyme's affinity and maximum catalytic capacity for L-Met substrate concentration, respectively.

Molecular weight determination

By SDS polyacrylamide gel electrophoresis

Polyacrylamide gel electrophoresis (PAGE) was used to evaluate the purity of L-Met isolated from *P. aeruginosa*. The protein profile analysis showed a single band following the gel filtration stage, demonstrating the excellent purity of the enzyme. The purified L-Met had a molecular weight of roughly 55 kDa.

Effect of some ionic factors on L-met activity

The Nesslerization method was used to measure the activity of the enzyme L-Met. An hour was spent at 30°C incubating the reaction mixture containing 1% L-methionine, potassium phosphate buffer, pyridoxal phosphate (PLP), and crude enzyme. The Nessler reagent

was used to measure the ammonia leak after the reaction was stopped. The enzyme's specific activity, which demonstrated good activity under these circumstances, was measured in µmol of ammonia generated per minute per mg of protein.

The L-Met enzyme's residual activity following exposure to several chemicals, each at a concentration of 5 mM, is shown in Table 3. The activity of the control enzyme remained at 100%. The enzyme activity was lowered to 70% by NaNO3 and CuCl2, suggesting a mild inhibitory action. 90% of the enzyme's residual activity was produced by CaCl2, indicating a mild inhibition. The enzyme maintained 100% activity in the presence of MnCl2 and KCl, indicating that these chemicals had no inhibitory effect.

Table 3. Effect of Various Reagents on the Activity of L-Met Enzyme

Reagent	Concentration (mM)	Remaining activity (%)
Control (Enzyme)		100
NaNO3	5	70
$CaCl_2$	5	90
$CuCl_2$	5	70
$MnCl_2$	5	100
KCl	5	100

L-Met cytotoxicity effect on cancer cell lines

MTT Assay: HCT-116 and A498 cancer cell lines were used to test the cytotoxicity of L-Met. The cells were cultured in a range of enzyme concentrations from 25 to 400 µg/mL. According to the MTT assay, L-Met exhibits dose-dependent activity. The concentration at which 50% inhibition of cell viability was found is represented by the IC_{50} value. The therapeutic effectiveness of the enzyme is highlighted by the fact that formazan crystal production was quantified by measuring its absorbance at 575 nm.

Cytotoxic effect of L-met on colorectal cancer cell line

Cytotoxic effects of treatments were assessed using the HCT-116 cell lines in different concentrations from 400 to 12.5 µg/mL. These, as summarized in Table 4, showed that Mean Diff. consistently showed significant cytotoxic effects at high concentrations through p-values below the 0.05 threshold. At 400 µg/mL, the Mean Diff. was 31.7130 (95% CI: 29.0600 to 34.3700), with a highly significant p-value of 0.0007. Similarly, at 200 µg/mL, the Mean Diff. was 32.6000 (95% CI: 29.0400 to 36.1600), confirming substantial cytotoxicity.

With the decrease in concentration, the Mean Diff. decreased, indicating a dose-dependent response. For example, at 100 µg/mL, the Mean Diff. was 26.9287 (95% CI: 24.0300 to 29.8300, *P*=0.0000). Even low concentrations, such as 25 µg/mL, showed significant effects with a Mean Diff. of 8.4497 (95% CI: 5.3600 to 11.5400, *P*=0.0009). However, at the lowest concentration of 12.5 µg/mL, the results were not significant, with a Mean Diff. of 1.6207 (95% CI: -0.2400 to 3.4800, p = 0.0753). (Figure 8).

Table 4. Dunnett's Multiple Comparisons Test Results in HCT-116

Concentration (µg/mL)	Mean Diff.	95% CI of Diff.	Statistical Significance	Summary	Adjusted *P*
400	31.713	29.0600 to 34.3700	Yes	Significant	0.0007
200	32.6	29.0400 to 36.1600	Yes	Significant	0.00005
100	26.9287	24.0300 to 29.8300	Yes	Significant	0.008
50	19.0973	15.0200 to 23.1800	Yes	Significant	0.0001
25	8.4497	5.3600 to 11.5400	Yes	Significant	0.0009
12.5	1.6207	-0.2400 to 3.4800	No	Not Significant	0.0753

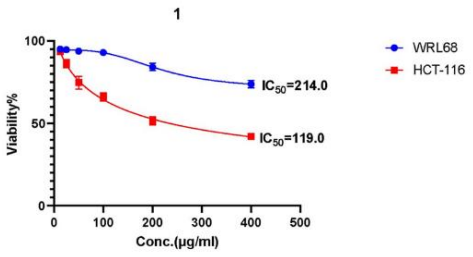

Figure 8. Dose-response curves for the L-Met treatment of the normal cell line WRL68 and HCT-116

Cytotoxic effect of L-Met on renal cell carcinoma cell line

When A498 cell lines were analyzed under the same conditions, different results were obtained (Table 5). With a non-significant p-value of 0.5655, the Mean Difference was -0.8873 (95% CI: -4.6000 to 2.8200) at the maximum concentration of 400 µg/mL. At 200 µg/mL, comparable non-significant outcomes were noted, with a Mean Difference of -1.1190 (95% CI: -3.5600 to 1.3200, *P*=0.2914).

At 100 µg/mL, notable cytotoxic effects were seen, with a Mean Diff. of 2.5073 (95% CI: 0.8500 to 4.1600, *P*=0.0115). The effects were continuously non-significant at concentrations of 50 µg/mL and lower, including 25 µg/mL (Mean Diff.= -0.5013, 95% CI: -2.2100 to 1.2100, p = 0.4852) and 12.5 µg/mL (Mean Diff. = -1.0417, 95% CI: -2.7900 to 0.7000, *P*=0.1858). (Figure 9).

Table 5. Dunnett's Multiple Comparisons Test Results in A498

Concentration (Âµg/mL)	Mean Diff.	95% CI of Diff.	Statistical Significance	Summary	Adjusted *P*
400	-0.8873	-4.6000 to 2.8200	No	Not Significant	0.5655
200	-1.119	-3.5600 to 1.3200	No	Not Significant	0.2914
100	2.5073	0.8500 to 4.1600	Yes	Significant	0.0115
50	-0.193	-1.0300 to 0.6400	No	Not Significant	0.5786
25	-0.5013	-2.2100 to 1.2100	No	Not Significant	0.4852
12.5	-1.0417	-2.7900 to 0.7000	No	Not Significant	0.1858

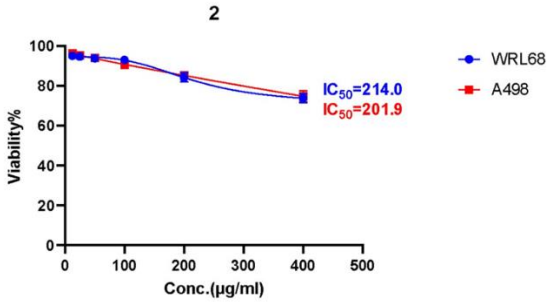

Figure 9. Dose-response curves for the L-Met treatment of the normal cell line WRL68 and A498

A comparison of the cytotoxic effects of L-Met on the normal liver cell line WRL68 and the cancer cell lines HCT-116 (colorectal carcinoma) and A498 (renal cell carcinoma) reveals a significant difference in sensitivity. As shown in Figure 8, WRL68 cells exhibited minimal cytotoxicity, with no significant effects observed even at higher concentrations of L-Met, suggesting a high degree of selectivity for cancerous cells.

In contrast, HCT-116 cells showed a strong dose-dependent cytotoxic response, with significant toxicity observed at concentrations as low as 25 µg/mL. Notably, A498 cells exhibited less sensitivity to L-Met, with significant cytotoxic effects only at 100 µg/mL, and no significant toxicity observed at concentrations below this level.

Discussion

Methionine dependence is a unique metabolic hallmark in cancer cells, representing a critical vulnerability to be targeted for therapeutic intervention. Methionine is essential for various cellular processes, such as DNA and histone methylation, redox regulation, and protein synthesis, all upregulated in cancer cells to sustain their rapid proliferation. Unlike normal cells, cancer cells have a defective ability to synthesize methionine de novo and instead rely on exogenous sources, a phenomenon referred to as "methionine dependence" (15,16).

The present study successfully characterized the L-Methioninase (L-Met) enzyme from Pseudomonas aeruginosa, optimizing its purification and assessing its biochemical properties, stability, and cytotoxic effects on

cancer cell lines. Our findings indicated significant growth inhibition in HCT-116 (CRC) and A498 (RCC) cell lines treated with L-Met. The respective IC_{50} values support the selective cytotoxic action of L-Met against tumor cells, given that the IC_{50} of regular cells-for example, WRL 68-reached as high as 214.0 µg/mL. Such a difference in sensitivity is consistent with several prior reports demonstrating the peculiar susceptibility of specific methionine-dependent malignant cells.

The dependency of cancer cells on methionine is due to their higher metabolic requirements. Methionine is the precursor for S-adenosylmethionine (SAM), the methyl donor for methylation reactions that control gene expression and chromatin structure (17,18). The high demand for SAM in cancer cells creates a bottleneck in methionine metabolism, which makes them specifically sensitive to methionine depletion (19). These observations are further supported by our study, in which disrupted methylation homeostasis after treatment with L-Met resulted in cancer cell death.

Besides, methionine metabolism interacts with redox regulation through the transsulfuration pathway, producing glutathione, a key antioxidant. Impaired methionine metabolism compromises redox homeostasis and further sensitizes the cancer cells to oxidative stress. This dual disruption of methylation and redox balance underlines methionine's central role in cancer cell survival (20).

Our data also highlights methionine depletion as a strategy to potentiate traditional therapies. The previous works have shown that methionine restriction enhances the cytotoxicity of 5-fluorouracil and cisplatin (19). Methionine deprivation impairs DNA synthesis and repair pathways, which are exceptionally vital for rapidly dividing cancer cells. The combination of methionine depletion and 5-FU in CRC models has significantly enhanced tumor regression. The synergistic action of L-Met with existing therapies offers a prospect for dose reduction of chemotherapeutic agents, thereby reducing systemic toxicity while maintaining efficacy. Future studies could explore the integration of L-Met with immune checkpoint inhibitors, given the emerging evidence linking metabolic reprogramming to immune evasion in the tumor microenvironment (21).

Clinical translation of L-Met therapy faces several challenges despite its promise. Therapeutic efficacy was critically dependent on enzyme stability and appropriate delivery. It has been demonstrated that conjugation of the enzyme L-Met with polyethylene glycol (PEGylation) extends the circulating half-life of L-Met and decreases its immunogenicity, as seen by Tan *et al*., (19). Furthermore, nanoparticle-based delivery systems offer a logical approach toward achieving tumor-specific targeting and sustained methionine depletion.

The metabolic flexibility of normal cells provides a therapeutic window for L-Met. Normal cells compensate for methionine depletion through homocysteine recycling, enabling selective toxicity toward cancer cells (22). However, identifying patients with methionine-dependent tumors remains a critical step. Metabolomic profiling and genetic analyses could help stratify patients based on their tumor's metabolic phenotype. Changes in enzymes involved in the methionine cycle, such as AHCY or adenosylhomocysteinase and methionine adenosyltransferase or MAT2A, serve as very reliable predictors of methionine dependence (20).

Colorectal cancer is one of the most common causes of tumor-related deaths worldwide. Metabolic reprogramming in CRC involves the upregulation of methionine cycle enzymes and dysregulation of pathways such as mTOR and PI3K-Akt, critical to sustaining tumor growth. Methionine depletion disrupts these pathways, thereby impairing tumor progression (23).

Similar is RCC, which bears mutations in genes like von Hippel-Lindau, stabilizing hypoxia-inducible factors that drive metabolic reprogramming. Methionine dependence in RCC opens a window of opportunity for a unique therapeutic target, as our findings have replicated and were previously shown by Xuliang Wang *et al*., (22). The sensitivity of A498 cells to L-Met underlines its possible use in overcoming the therapeutic challenges posed by RCC's resistance to conventional therapies.

Our study successfully characterized and purified L-Met, elucidating its enzymatic properties and demonstrating its cytotoxic potential against colorectal cancer cells. The findings demonstrated strong cytotoxic activity against colorectal cancer cells, whereas activity against renal cell carcinoma cells was lower or remained inconclusive.

Further research is needed to optimize dosing regimens and delivery mechanisms to maximize therapeutic benefits. Integrating metabolomics and genomics into clinical workflows could enhance patient selection and predict therapeutic responses. Additionally, exploring the role of methionine metabolism in immune modulation could open new avenues for combination therapies involving L-Met and immune checkpoint inhibitors.

Acknowledgements

The authors thank the University of Babylon, for their

generous support in providing necessary laboratory equipment and facilitating suitable facilities.

References

1. Sun S-n, Hu S, Shang Y-p, Li L-y, Zhou H, Chen J-s, et al. Relevance function of microRNA-708 in the pathogenesis of cancer. Cell Signal 2019;63:109390.
2. Sharma R, Kannourakis G, Prithviraj P, Ahmed N. Precision medicine: an optimal approach to patient care in renal cell carcinoma. Front Med 2022;9:766869.
3. Jin H, Wang L, Bernards R. Rational combinations of targeted cancer therapies: background, advances and challenges. Nat Rev Drug Discov 2023;22:213-34.
4. Qoura LA, Balakin KV, Hoffman RM, Pokrovsky VS. The potential of methioninase for cancer treatment. Biochim Biophys Acta Rev Cancer 2024:189122.
5. Bin P, Wang C, Zhang H, Yan Y, Ren W. Targeting methionine metabolism in cancer: opportunities and challenges. Trends Pharmacol Sci 2024;45:395-405.
6. Sanderson SM, Gao X, Dai Z, Locasale JW. Methionine metabolism in health and cancer: a nexus of diet and precision medicine. Nat Rev Cancer 2019;19:625-37.
7. Maggi M, Scotti C. Enzymes in metabolic anticancer therapy. Therapeutic Enzymes: Function and Clinical Implications 2019:173-99.
8. Javia BM, Gadhvi MS, Vyas SJ, Ghelani A, Wirajana N, Dudhagara DR. A review on L-Met in cancer therapy: Precision targeting, advancements and diverse applications for a promising future. Int J Biol Macromol 2024:130997.
9. Mármol I, Sánchez-de-Diego C, Pradilla Dieste A, Cerrada E, Rodriguez Yoldi MJ. Colorectal carcinoma: a general overview and future perspectives in colorectal cancer. Int J Mol Sci 2017;18:197.
10. Mohd AB, Ghannam RA, Mohd OB, Elayan R, Albakri K, Huneiti N, et al. Etiologies, gross appearance, histopathological patterns, prognosis, and best treatments for subtypes of renal carcinoma: an educational review. Cureus 2022;14.
11. Chen J, Cui L, Lu S, Xu S. Amino acid metabolism in tumor biology and therapy. Cell Death & Disease 2024;15:42.
12. Gutiérrez-Salmerón M, Lucena SR, Chocarro-Calvo A, García-Martínez JM, Orozco RMM, García-Jiménez C. Metabolic and hormonal remodeling of colorectal cancer cell signalling by diabetes. Endocr Relat Cancer 2021;28:191-206.
13. Mazumder S, Higgins PJ, Samarakoon R. Downstream targets of VHL/HIF-α signaling in renal clear cell carcinoma progression: mechanisms and therapeutic relevance. Cancers 2023;15:1316.
14. Dhankhar R, Kawatra A, Mohanty A, Gulati P. Microbial enzymes used in prodrug activation for cancer therapy: insights and future perspectives. Current Protein and Peptide Science 2021;22:514-25.
15. Diala ES, Cheah MS, Rowitch D, Hoffman RM. Extent of DNA methylation in human tumor cells. J Natl Cancer Inst 1983;71:755-64.
16. Hoffman RM. Altered methionine metabolism, DNA methylation and oncogene expression in carcinogenesis: a review and synthesis. BBA Reviews on Cancer 1984;738:49-87.
17. Michalak EM, Burr ML, Bannister AJ, Dawson MA. The roles of DNA, RNA and histone methylation in ageing and cancer. Nat. Rev Mol Cell Biol 2019;20:573-89.
18. Erichsen L, Thimm C, Santourlidis S. Methyl group metabolism in differentiation, aging, and cancer. Int J Mol Sci 2022;23:8378.
19. Tan Y, Xu M, Hoffman RM. Broad selective efficacy of recombinant methioninase and polyethylene glycol-modified recombinant methioninase on cancer cells in vitro. Anticancer Res 2010;30:1041-6.
20. Vande Voorde J, Steven RT, Najumudeen AK, Ford CA, Dexter A, Gonzalez-Fernandez A, et al. Metabolic profiling stratifies colorectal cancer and reveals adenosylhomocysteinase as a therapeutic target. Nat Metab 2023;5:1303-18.
21. Liu S, Locasale JW. Delineating a role for methionine metabolism in colorectal cancer. Cancer Res 2023;83:3833-4.
22. Wang X, Guo X, Yu W, Li C, Gui Y, Cai Z. Expression of methionine adenosyltransferase 2A in renal cell carcinomas and potential mechanism for kidney carcinogenesis. BMC cancer. 2014;14:1-9.
23. Garg S, Miousse IR. Rescue of Methionine Dependence by Cobalamin in a Human Colorectal Cancer Cell Line. Nutrients 2024;16:997.